Mechanical and Transport Properties of Coextruded Films

Y. J. KIM, C. D. HAN, B. K. SONG, and E. KOUASSI, *Department of Chemical Engineering, Polytechnic Institute of New York, Brooklyn, New York 11201*

Synopsis

Two-layer films were produced by using the blown-film coextrusion apparatus constructed in our laboratory. For this study, we have produced films of the following combinations: (1) LDPE/CXA 3095; (2) LDPE/Plexar 3; (3) LDPE/EMA; (4) nylon 6/LDPE; (5) nylon 6/CXA 3095; (6) nylon 6/Plexar 3; (7) nylon 6/EMA. Tensile properties of the coextruded films were measured with an Instron testing machine, and correlated to processing variables, namely, takeup ratio and blowup ratio. From tensile property measurements, we have found that both the ultimate tensile strength and the tensile modulus of coextruded films follow the additivity rule with respect to the volume fraction of the individual components. With the films produced, we also conducted dynamic mechanical measurements with the aid of a Rheovibron Dynamic Viscoelastometer DDV-II, and attempted to test the Zorowski–Murayama theory to determine the adhesion characteristics of the coextruded films. Furthermore, permeability of the coextruded films to gases (namely, N_2, O_2, and CO_2) was measured by using a pressure differential apparatus constructed in our laboratory. We have found that the permeability of composite films follows the inverse additivity rule, i.e., the reciprocal of the permeability of composite film is given by the sum of the reciprocals of the permeabilities of the individual layers.

INTRODUCTION

In recent years, the packaging and container industries have paid increasing attention to the development of new or improved products by means of coextrusion processes. Representative commercial products available in the market, produced by coextrusion, are multilayer flat films, multilayer blown films, sandwiched foam composites, etc. Depending on the end-use properties required and the availability of polymer combinations suitable for specific applications, the packaging industry, for instance, produces two-, three-, or five-layer coextruded films, using chemically dissimilar polymers. Needless to say, two-layer films are more economical, and easier to produce, than three-layer films, if one can achieve the same objective by using two dissimilar polymers. However, one often encounters the situation in which the two polymers chosen have rather poor adhesion at the interface, while possessing all the other properties required for the specific application. In such a situation, one must find a third component that may be used as an adhesive layer between the two polymers. One such example of commercial importance is the polyethylene/polyamide coextrusion system.

Polyethylene is used in some food packaging applications. Its cost, strength, barrier properties to moisture, and ease of fabrication make it ideal for numerous applications. Its lack of barrier properties to aromatics

Journal of Applied Polymer Science, Vol. 29, 2359–2382 (1984)
 CCC 0021-8995/84/072359-24$04.00

and oils bars it from many other potential applications. On the other hand, polyamides are very strong, easily fabricated and possess excellent barrier properties to aromatics and oils, but have poor barrier properties to moisture. Therefore, a combination of polyethylene and polyamide (e.g., nylon 6) is very attractive for many demanding applications, including food packaging. However, there is rather poor adhesion at the interface between the polyethylene and polyamide layers in coextruded films. For this reason, in recent years, serious efforts[1-3] have been made by industry to develop adhesive polymers that may be coextruded with polyethylene and polyamide. As a result of such efforts, a series of adhesive polymers for some specific applications have now been placed on the market by Chemplex Co. and DuPont Co.

Multilayer films have been commercially produced by means of either the blown-film coextrusion process or flat-film coextrusion process. The blown-film coextrusion process has one advantage, among others, over the flat-film coextrusion process in that biaxially oriented film can be produced in a one-step operation. The recent monograph by Han[4] describes the fundamental aspects of coextrusion processes, with emphasis on the importance of the rheological properties of the individual polymers to be selected, from the points of view of designing coextrusion dies and avoiding interfacial flow instability. In more recent studies, Han and co-workers have investigated the rheological aspects of interfacial flow instability in two-layer flat-film coextrusion,[5] the three-layer sandwich flat-film coextrusion process,[6] and the nonisothermal two-layer flat-film coextrusion process.[7]

As part of our continuing efforts to enhance our understanding of multilayer film coextrusion processes, we have very recently carried out a study of the blown-film coextrusion process. The primary objective of the study was, first, to prepare film samples under a variety of well-controlled processing conditions and, then, to determine the mechanical and transport properties of the coextruded film samples. In this paper, we shall report the highlights of our findings.

EXPERIMENTAL

Materials. The polymers used in the coextrusion experiments were: (1) low-density polyethylene (LDPE) (Dow Chemical, PE529); (2) ethylene–methyl acrylate copolymer (EMA) (Gulf Chemicals, Poly-Eth 2255); (3) nylon 6 (Allied Chemical, Capron 8209F); (4) chemically modified polyolefin (Chemplex, Plexar 3); (5) ethylene-based multifunctional polymer (DuPont, CXA 3095). The rheological properties of these polymers are reported in one of our previous papers.[5]

The pairs of polymers chosen for coextruding two-layer films were: (a) nylon/LDPE; (b) nylon/CXA; (c) nylon/Plexar; (d) nylon/EMA; (e) LDPE/CXA; (f) LDPE/Plexar; (g) LDPE/EMA. These combinations were chosen so that we could predict the mechanical and transport properties of the following three-layer systems, (a) LDPE/CXA/nylon, (b) LDPE/Plexar/nylon, (c) LDPE/EMA/nylon, without necessarily producing these three-layer films by coextrusion. It should be mentioned that both CXA 3095 and Plexar 3 are on the market for use as adhesive resins for coextruding with nylon and polyethylene.

Apparatus and Experimental Procedure Employed for Blown-Film Coextrusion. The apparatus consists of a die, two extruders, a cooling ring, and a take-up device. A schematic of the die is given in Figure 1. It was designed to receive two feed streams–one entering into the inner annulus and the other into the outer annulus—so that when the two melt streams meet at the entrance of the straight flow channel, they form two concentric layers while flowing together through the annular flow channel (i.e., die land).

The straight section of the annular flow channel has the following dimensions: inner diameter 3.81 cm, die opening 0.159 cm, and length 2.54 cm. In the die land, six melt pressure transducers are mounted along the die axis, which permits us to determine the pressure gradient and hence the wall shear stress in the die. Such information is essential for understanding the performance of the die in terms of the pressure drops required and, also, for relating the rheological properties of the polymers to coextrudability. Upon exiting from the die, the two-layer film was inflated with air and stretched by a take-up device.

During the experiment, the following variables were measured: (1) the mass flow rate of the individual melt streams (hence the linear velocity of the melt at the die lip); (2) the diameter of the tubular bubble (thus, blowup ratio); (3) the speed of the takeup device (thus, takeup ratio); (4) the pressure distribution along the die axis (thus, wall shear stress); (5) the thickness of the tubular blown film.

Tensile Property Measurement. Tensile properties of the coextruded samples were determined at room temperature, using an Instron testing machine. The ultimate tensile strength, the tensile modulus, and the elon-

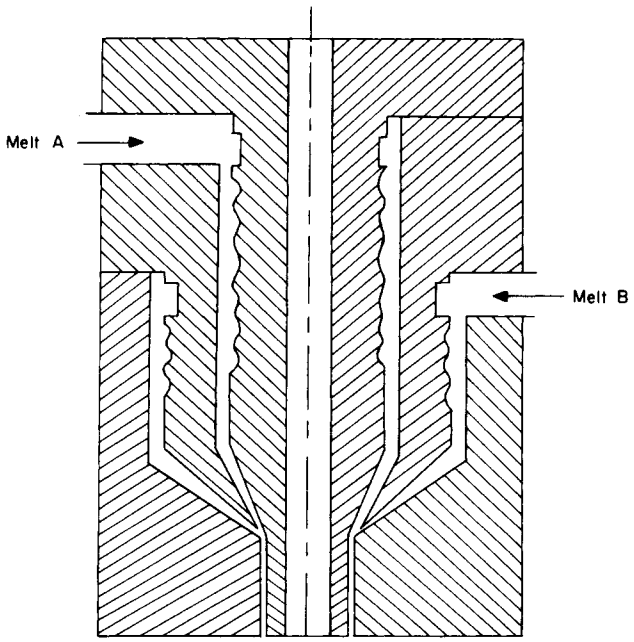

Fig. 1. Schematic of the blown-film coextrusion die employed.

gation at break were determined from the tensile stress-strain curves. The cross head speed was 2.54 cm/min. Measurements were taken on several samples collected under identical processing conditions, and the average value was calculated.

Dynamic Mechanical Measurement. Dynamic mechanical properties were determined, using a Rheovibron dynamic viscoelastometer (Model DDV-II, Toyo Measuring Instruments Co., Tokyo, Japan). Measurements were taken on film samples at a frequency of 110 Hz and at temperatures ranging from −20°C to 100°C. Film samples were collected under identical processing conditions, i.e., at the same extrusion melt temperature (240°C) and same total volumetric flow rate (0.529 cm^3/s). The dimensions of typical film samples employed were 0.35 cm × 0.035 cm × 4 cm.

When the sample reached an equilibrium temperature, it was heated at the rate of 1.5°C. Measurements were taken on several samples collected under identical processing conditions in order to ascertain the reliability of the data.

Gas Permeability Measurement. Gas permeability measurements were taken, using a pressure differential apparatus, constructed in our laboratory, which is essentially the same as that described in ASTM D 1876-61T. The apparatus consists of a test cell, gas feed system, downstream constant volume cavity, a pressure transducer, a recorder, a Heiss gauge, and a rupture disk. The apparatus was placed in a constant temperature chamber with sliding doors. The temperatures chosen for measurement were 20°C, 15°C, 10°C, and 0°C.

The blown film samples were cut to a size of about 4 cm in diameter and were edged with adhesive-backed aluminum tape, so that the central circular areas (3 cm in diameter) could be exposed to the permeation of gas. The sample was sandwiched between discs of sintered metal, to prevent it from sagging, and clamped between O-rings. The gases used for permeability measurements were nitrogen (N_2), oxygen (O_2), and carbon dioxide (CO_2).

A vacuum pump was used to evacuate the system down to a pressure of about 0.3 mm Hg, and a test gas was run in the upstream section up to 90 psig, which was the maximum pressure allowed by the regulator used. The entire system was evacuated between runs, and three runs were run for a given combination of film and gas. The experimental procedure employed was essentially the same as described in ASTM D 1876-61T.

RESULTS AND DISCUSSION

Tensile Properties of Coextruded Films. Figure 2 shows stress–strain curves for nylon 6, Plexar 3, and coextruded nylon 6/Plexar 3 films. It is seen in Figure 2 that the nylon 6 film sample shows a yield stress at a certain value of strain. As the strain increases after the stress passes the yield value, the stress first decreases and then attains a minimum value. During this period, we observed that either the width of the film sample narrowed or necking occurred. After this, until the film sample broke down during further stretching, so-called cold drawing takes place. In other words, the molecular chains of nylon 6 are stretched locally in the tensile direction, resulting in no further change in the cross-sectional area of the film sample.

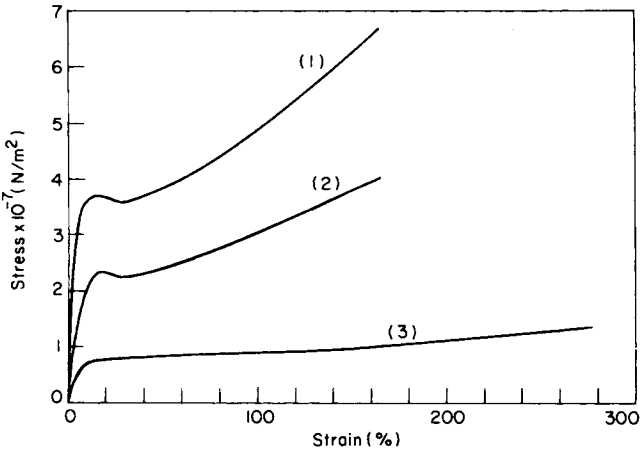

Fig. 2. Stress–strain curves for: (1) nylon 6; (2) nylon 6/Plexar 3 = 51.7/48.3 (vol %); (3) Plexar 3. The processing conditions employed for obtaining the film samples are: BUR = 1.8; TUR = 1.9; total flow rate = 0.529 cm^3/s; melt extrusion temperature = 240°C.

On the other hand, the Plexar 3 film sample shows the flow characteristic of rubbery materials. It is seen in Figure 2 that neither yield stress nor a stress minimum occurs for this sample. Consequently, Plexar 3 has a low modulus, but very high elongation at break, approximately 275%. It should be noted that, as the strain increases, little increase in stress takes place.

It is also seen in Figure 2 that the stress–strain curve of the nylon 6/Plexar 3 sample lies between that of nylon 6 and Plexar 3. Note that the elongation at break of the coextruded nylon 6/Plexar 3 film sample is almost the same as that of the nylon 6 film sample. This seems to indicate that Plexar 3 does not help in preventing the failure of the nylon 6/Plexar 3 film sample; that is, the failure of the coextruded nylon 6/Plexar 3 film sample does not seem to be affected by the presence of Plexar 3.

Figure 3 gives plots of the ultimate tensile strength in both the machine

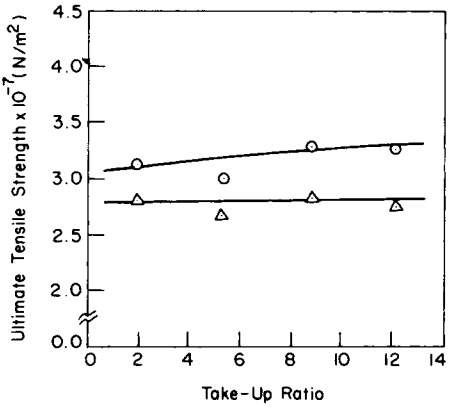

Fig. 3. Ultimate tensile strength vs. takeup ratio for the nylon 6/Plexar 3 = 35/65 (vol %) system. The processing conditions employed are the same as in Figure 2, except the TUR: (⊙) MD; (△) TD.

direction (MD) and transverse direction (TD) vs. takeup ratio (TUR), and Figure 4 gives plots of the ultimate tensile strength in both the MD and TD vs. blowup ratio (BUR), of the coextruded nylon 6/Plexar 3 film sample. It should be noted that the film samples used for the tensile property measurements were collected under identical processing conditions, i.e., at the same extrusion temperature (240°C) and same total volumetric flow rate (0.529 cm^3/s). It is seen in Figure 3 that the ultimate TD tensile strength seems to increase *little* with TUR, whereas the ultimate MD tensile strength increases moderately with TUR. On the other hand, the ultimate tensile strength in both the MD and TD increases with BUR, as may be seen in Figure 4. Note in Figures 3 and 4 that the ultimate MD tensile strength always exceeds the TD tensile strength.

It is a well-known fact that films (or fibers) should be stretched at a temperature slightly above their glass transition temperature (T_g), in order to make them fully oriented and achieve an increase in mechanical properties. Note that the data in Figure 3 represent coextruded nylon 6/Plexar 3 films stretched at about 238°C. Note further that the molecules of nylon 6 and Plexar 3 can be neither oriented nor crystallized at that temperature, because the stresses built into the film, while being stretched, were instantly relaxed because of the high stretching temperature employed. On the other hand, the coextruded nylon 6/Plexar 3 film samples, used for generating the data given in Figure 4, were stretched at a temperature much lower than 238°C. It should be mentioned that the nylon 6 underwent molecular orientations when the coextruded film samples were stretched during tensile property measurements. The molecular orientations occurring during the tensile property measurements should be distinguished from those that

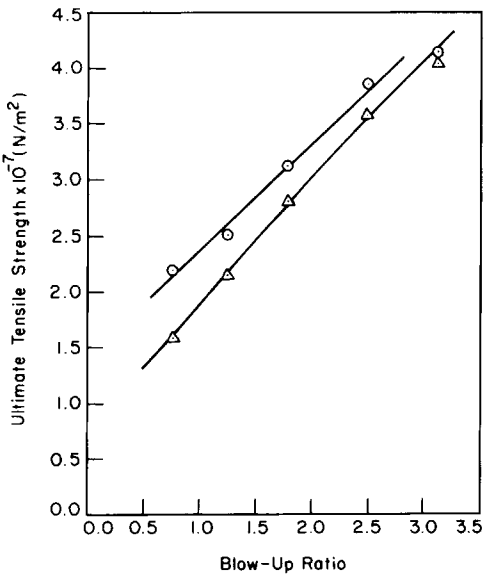

Fig. 4. Ultimate tensile strength vs. blowup ratio for the nylon 6/Plexar 3 = 35/65 (vol %) system. The processing conditions employed are the same as in Figure 2, except the BUR: (⊙) MD; (△) TD.

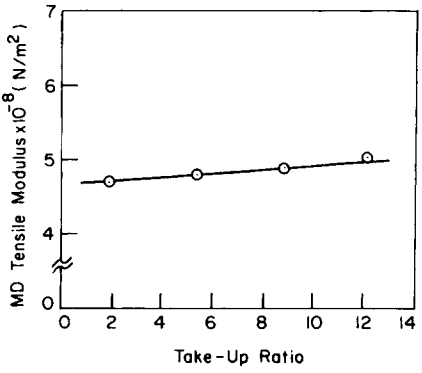

Fig. 5. Tensile modulus in the machine direction vs. takeup ratio for the nylon 6/Plexar 3 = 35/65 (vol %) system. The processing conditions employed are the same as in Figure 2, except the TUR.

might have occurred during the sample preparation in the coextrusion operation. In other words, it is difficult to correlate directly the tensile properties of the coextruded films with processing conditions, unless the extent of the molecular orientations, introduced during the processing of the film, is distinguished from that introduced during the tensile testing experiment.

Figure 5 gives plots of MD tensile modulus vs. TUR, and Figure 6 gives plots of TD tensile modulus vs. BUR. It is seen in Figures 5 and 6 that the MD tensile modulus increases slowly with TUR, whereas the TD tensile modulus increases significantly with BUR. These results are consistent with those shown in Figures 3 and 4.

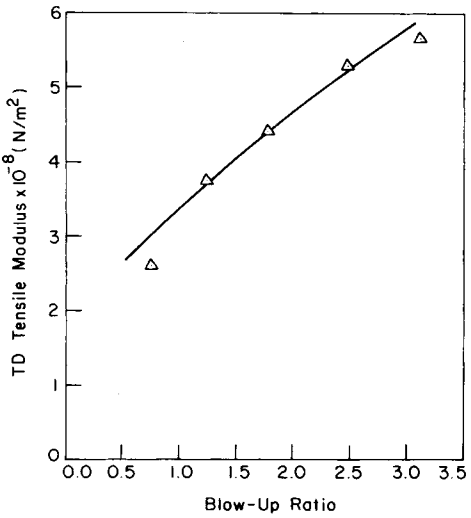

Fig. 6. Tensile modulus in the transverse direction vs. blowup ratio for the nylon 6/Plexar 3 = 35/65 (vol %) system. The processing conditions employed are the same as in Figure 2, except the BUR.

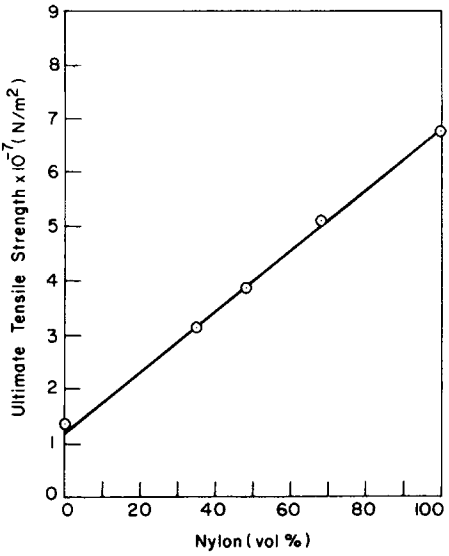

Fig. 7. Ultimate tensile strength vs. vol % of nylon 6 in the nylon 6/Plexar 3 coextrusion system. The processing conditions employed are the same as in Figure 2.

Figure 7 shows plots of MD ultimate tensile strength vs. volume percent of nylon 6, and Figure 8 plots of MD tensile modulus vs. volume percent of nylon 6, for coextruded nylon 6/Plexar 3 film samples. Figure 9 gives plots of MD ultimate tensile strength vs. volume percent of Plexar 3, and Figure 10 plots of MD tensile modulus vs. volume percent of Plexar 3, for coextruded LDPE/Plexar 3 film samples. Also, Figure 11 gives plots of MD elongation at break vs. volume percent of nylon 6 for coextruded nylon 6/ Plexar 3 film samples, and Figure 12 plots of MD elongation at break vs. volume percent of Plexar 3 for coextruded LDPE/Plexar 3 film samples.

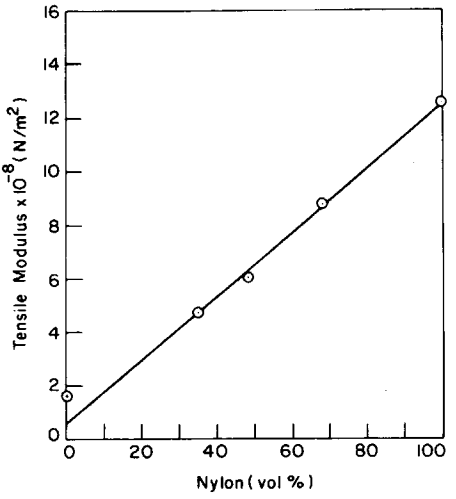

Fig. 8. Tensile modulus vs. vol % of nylon 6 in the nylon 6/Plexar 3 coextrusion system. The processing conditions employed are the same as in Figure 2.

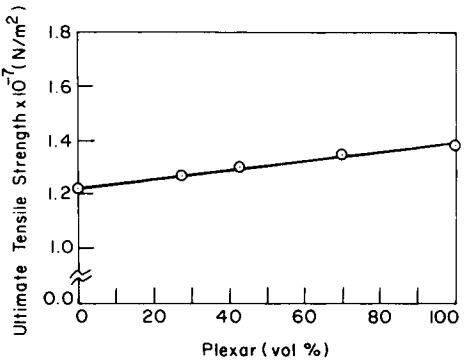

Fig. 9. Ultimate tensile strength vs. vol % of Plexar 3 in the LDPE/Plexar 3 coextrusion system. The processing conditions employed for obtaining the film samples are: BUR = 2.2; TUR = 1.9; total flow rate = 0.529 cm^3/s; melt extrusion temperature = 200°C.

As may be seen in Figures 7–12, the ultimate tensile strength and tensile modulus follow the additivity rule, whereas the elongation at break does not. These results are in good agreement with the study of Schrenk and Alfrey.[8] It is of interest to note that the elongation at break decreases rapidly with increasing the nylon 6 content and levels off at about 40 vol % of nylon 6 in the nylon 6/Plexar 3 system, as shown in Figure 11, whereas the elongation at break increases with the Plexar 3 content and goes through a maximum at about 70 vol % of Plexar 3 in the LDPE/Plexar 3 system, as shown in Figure 12.

It can be concluded from the results given in Figures 7–10 that we can now predict the ultimate tensile strength and tensile modulus of the three-layer systems, namely, LDPE/CXA 3095/Nylon 6 and LDPE/Plexar 3/nylon 6 systems, without necessarily producing these three-layer films by coextrusion.

Dynamic Mechanical Behavior of Coextruded Films. Figures 13–16 describe the temperature dependence of dynamic moduli (E' and E'') and loss tangent (tan δ) of the LDPE/CXA 3095, LDPE/Plexar 3, nylon 6/CXA 3095, and nylon 6/Plexar 3 systems. Note in these figures that the storage

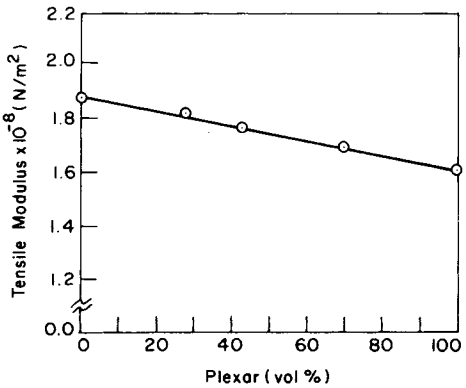

Fig. 10. Tensile modulus vs. vol % of Plexar 3 in the LDPE/Plexar 3 coextrusion system. The processing conditions employed are the same as in Figure 9.

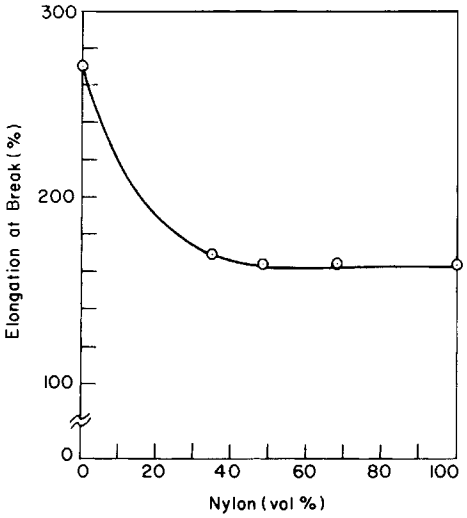

Fig. 11. Elongation at break vs. vol % of nylon 6 in the nylon 6/Plexar 3 coextrusion system. The processing conditions employed are the same as in Figure 2.

modulus E' and tan δ were measured directly, and the loss modulus E'' was calculated from the definition, tan $\delta = E''/E'$.

In the past, some attempts have been made to infer, from the relaxation spectra, the adhesion characteristics between adjacent layers in a coextruded film,[9] between polymers in heterogeneous polymer composites, and between a particulate filler and the matrix in filled polymers.[10–13] A quantitative approach to determining the adhesion characteristics between the

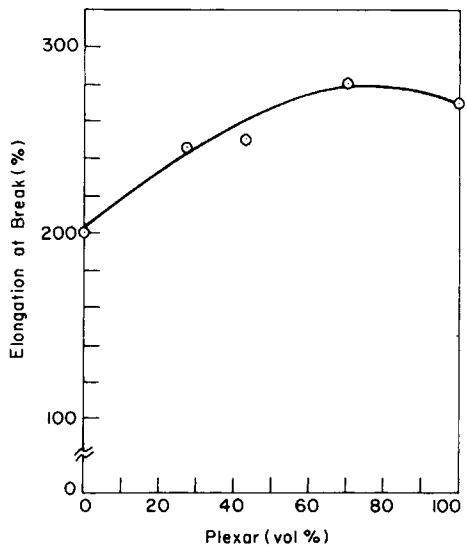

Fig. 12. Elongation at break vs. vol % of Plexar 3 in the LDPE/Plexar 3 coextrusion system. The processing conditions employed are the same as in Figure 9.

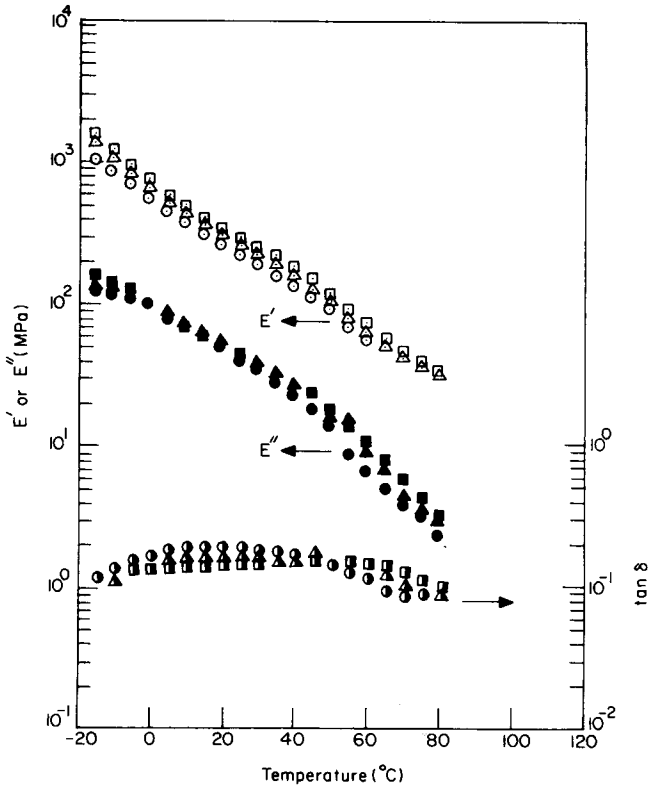

Fig. 13. Temperature dependence of dynamic moduli (E' and E'') and loss tangent (tan δ) of the LDPE/CXA 3095 system: (○,●,◑) LDPE; (□,■,◨) CXA 3095; (△,▲,◭) LDPE/CXA 3095.

two layers in a laminated composite was suggested by Zorowski and Murayama,[14] who derived the following expressions:

$$\tan \delta_{adh} = \tan \delta_{exp} - \tan \delta_s \tag{1}$$

$$\tan \delta_s = \frac{E_1 V_1 \tan \delta_1 + E_2 V_2 \tan \delta_2}{E_1 V_1 + E_2 V_2} \tag{2}$$

where $\tan \delta_{exp}$ is the experimentally determined *effective* loss tangent, defined as the ratio of the imaginary and real parts of the complex modulus, E''/E', and $\tan \delta$ is the loss tangent, E the modulus and V the volume fraction, the subscripts referring to components 1 and 2.

According to Zorowski and Murayama,[14] $\tan \delta_s$, defined by eq. (2), represents the effective loss tangent for the material under test with *perfect* adhesion. The experimentally measured value $\tan \delta_{exp}$ of a system (e.g., a two-layer film), if it has poor adhesion, would be greater than the value $\tan \delta_s$ that assumes perfect adhesion. The Zorowski–Murayama theory is based on the notion that a two-layer specimen having poor adhesion, when subjected to vibration parallel to the direction of major axis, would give

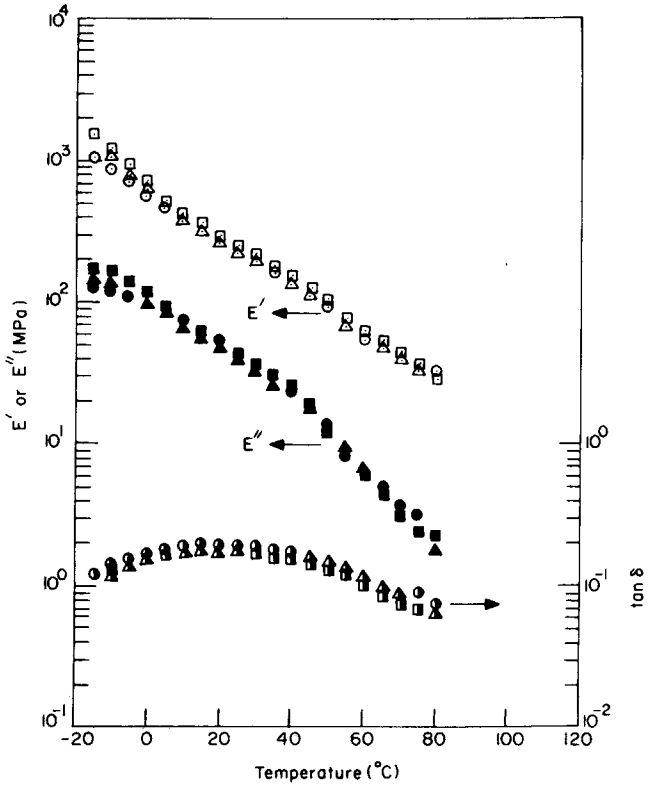

Fig. 14. Temperature dependence of dynamic moduli (E' and E'') and loss tangent (tan δ) of the LDPE/Plexar 3 system: (⊙,●,◑,) LDPE; (□,■,◧) Plexar 3; (△,▲,◭) LDPE/Plexar 3.

rise to greater energy dissipation (in terms of loss tangent) than the system having perfect adhesion.

Tables I–IV give representative results of our dynamic mechanical test in terms of tan δ_{adh} and the tan δ_{adh}/tan δ_s ratio. A close examination of the results of the dynamic mechanical test, displayed in Tables I and II, puzzled us somewhat, because *negative* values of tan δ_{adh} are obtained for the coextrusion systems investigated. If the various assumptions made in the derivation of eq. (2) are correct, and if, further, the notion that eq. (1) may be used as a measure of the adhesion characteristic of two-layer laminates is correct, tan δ_{adh} cannot become negative. This has prompted us to examine some of the assumptions made in the derivation of eq. (2).

A close examination of eq. (2) shows that the storage modulus E of the laminated composite (i.e., coextruded film in this study) must follow the linear additivity rule:

$$E = \sum_i E_i h_i / h \tag{3}$$

where E_i and h_i are the storage modulus and thickness of the individual layer, respectively, and h is the total layer thickness.

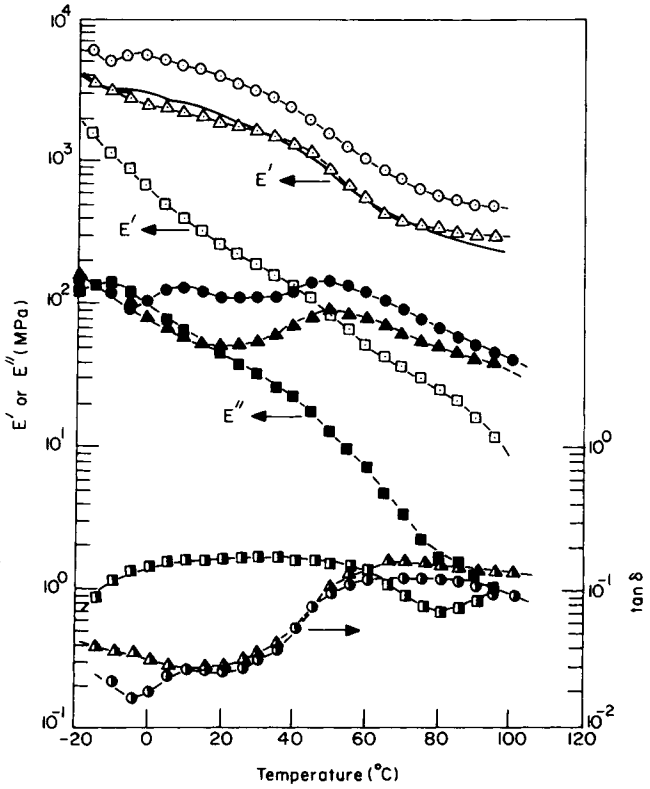

Fig. 15. Temperature dependence of dynamic moduli (E' and E'') and loss tangent (tan δ) of the nylon 6/CXA 3095 system: (⊙,●,◑) nylon 6; (□,■,◨) CXA 3095; (△,▲,◭) nylon 6/CXA 3095; (——) theoretical prediction of E' using a parallel model.

Figure 17 gives a comparison of the experimentally measured E' values and the theoretically calculated values of E' using a *parallel model* [i.e., eq. (3)], for the LDPE/Plexar 3 system. It is seen that the measured values of E' are greater than the calculated ones over the range of temperature investigated. In such situations, the values of tan δ_s defined by eq. (2) can be greater than the values of tan δ_{exp}, because tan δ_s also is based on the assumption of the linear additivity rule for the storage modulus. It appears therefore that *negative* values of tan δ_{adh} presented in Table II are in part related to the situation where the measured values of E' are greater than the theoretically predicted ones using a *parallel* model.

It is seen in Figure 15 that, for the nylon 6/CXA 3095 system, the measured values of E' are greater at temperatures below −10°C, and less at temperatures between −10°C and 80°C, than the theoretically predicted ones. It appears, again, that *negative* values of tan δ_{adh} presented in Table III are in part related to the situation where the measured values of E' are greater than the theoretically predicted ones using a *parallel* model.

On the other hand, Table IV shows that large positive values of tan δ_{adh}, relative to tan δ_s, are seen at temperatures above 20°C, which is an indication, according to the Zorowski–Murayama theory [i.e., eq. (1)], that nylon

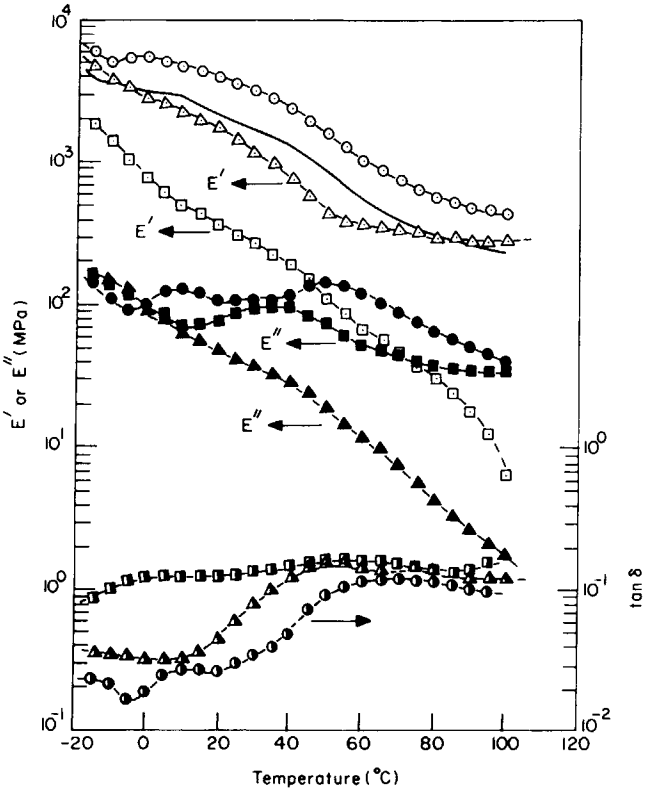

Fig. 16. Temperature dependence of dynamic moduli (E' and E'') and loss tangent (tan δ) of the nylon 6/Plexar 3 system: (⊙,●,◑) nylon 6; (⊡,■,◨) Plexar 3; (△,▲,◭) nylon 6/Plexar 3; (——) theoretical prediction of E' using a parallel model.

6 and Plexar 3 have poor adhesion. However, as given in Table V, an independent peel test demonstrates that they have very good adhesion at room temperature.[15]

A close examination of Figure 16 and Table IV reveals that, for the nylon 6/Plexar 3 system, even when the measured and calculated values of E' are very close to each other, *negative* values of tan δ_{adh} are still possible. Therefore, one may conclude that there must be some reasons, other than the assumption of the linear additivity rule for the storage modulus, that make the tan δ_{adh} values *negative*. It should be pointed out, however, that the values of tan δ given in Tables I–IV are rather small, and the difference between two small values is very difficult to determine with great accuracy. One can thus argue that the values of tan δ_{adh} given in Tables I–IV are too small to be of physical significance.

Nevertheless, we identified two areas of experimental difficulty, that may be inherent in the use of the Rheovibron Viscoelastometer for very thin film samples, in determining the absolute magnitude of tan δ. One is the possibility of slippage of the specimen from the clamps and consequently misalignment of the specimen in the grips. The other is the great sensitivity of the measured values of tan δ to the geometry (i.e., length/area ratio) of

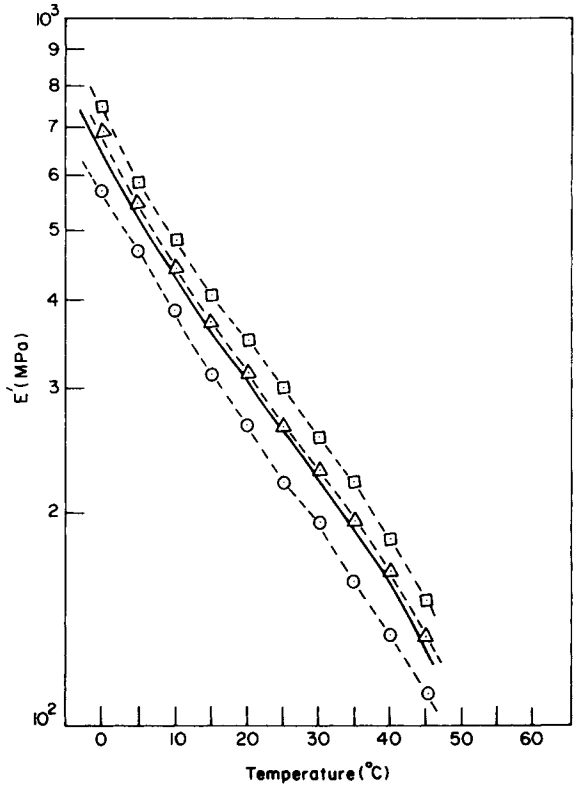

Fig. 17. Temperature dependence of storage modulus (E') of the LDPE/Plexar 3 system: (⊙) LDPE; (⊡) Plexar 3; (△) LDPE/Plexar 3. (——) represents the Theoretical prediction.

the specimen. More specifically stated, we observed that the tan δ_{exp} values scattered noticeably when the length/area ratio of the specimen was smaller than a certain critical value.

We therefore reached the conclusion that any attempt at using the Zorowski–Murayama theory for determining quantitatively the adhesion characteristics of coextruded films requires extreme caution.

Gas Permeability of Coextruded Films. Table VI gives a summary of gas permeabilities determined in our experiment. It is seen that, in all cases, the permeability increases in the following order: $CO_2 > O_2 > N_2$ and that nylon has low permeability and thus better barrier properties to the gases studied than LDPE, CXA 3095, or Plexar 3.

The temperature dependence of the permeability is demonstrated in Figure 18. Two things are worth noting: (1) the permeability follows the Arrhenius relationship; (2) the permeability of LDPE film increases with increasing temperature, whereas the permeability of nylon film decreases with increasing temperature. Note, however, that the permeability of the nylon/LDPE composite film is controlled primarily by the nylon film, as may be seen in Figure 19. This is due to the fact that the permeability of the nylon film is about one order of magnitude lower than the permeability of the LDPE film (see Table VI and Fig. 18).

TABLE I
Results of Dynamic Mechanical Test for the LDPE/CXA 3095 System

Temp (°C)	Measured $E' \times 10^{-9}$ (N/m^2)	Calculated $E' \times 10^{-9}$ (N/m^2)	tan δ_{exp}	tan δ_s	tan δ_{adh}	tan δ_{adh}/tan δ_s (%)
−20	1.714	1.506	0.095	0.100	−0.005	− 5.00
−15	1.472	1.317	0.103	0.112	−0.009	− 8.00
−10	1.128	1.044	0.122	0.136	−0.014	−10.29
− 5	0.824	0.825	0.142	0.155	−0.013	− 8.38
0	0.631	0.638	0.157	0.167	−0.010	− 5.98
5	0.481	0.500	0.177	0.177	0.000	0.00
10	0.377	0.403	0.177	0.181	−0.004	− 2.21
15	0.316	0.332	0.178	0.183	−0.005	− 2.73
20	0.264	0.275	0.179	0.183	−0.004	− 2.18
25	0.222	0.233	0.178	0.182	−0.004	− 2.19
30	0.187	0.202	0.176	0.178	−0.002	− 1.12
35	0.158	0.169	0.171	0.169	0.002	1.22
40	0.135	0.143	0.165	0.164	0.001	0.06
45	0.112	0.118	0.157	0.152	0.005	3.18

TABLE II
Results of Dynamic Mechanical Test for the LDPE/Plexar 3 System

Temp (°C)	Measured $E' \times 10^{-9}$ (N/m^2)	Calculated $E' \times 10^{-9}$ (N/m^2)	tan δ_{exp}	tan δ_s	tan δ_{adh}	tan δ_{adh}/tan δ_s (%)
−20	1.655	1.523	0.078	0.087	−0.009	−10.34
−15	1.441	1.323	0.093	0.097	−0.004	− 4.12
−10	1.143	1.035	0.116	0.121	−0.005	− 4.13
− 5	0.846	0.832	0.137	0.139	−0.002	− 1.44
0	0.693	0.647	0.148	0.156	−0.008	− 5.12
5	0.547	0.514	0.161	0.163	−0.002	− 1.22
10	0.444	0.428	0.167	0.165	0.002	1.21
15	0.373	0.350	0.169	0.167	0.002	1.19
20	0.317	0.299	0.169	0.168	0.001	0.59
25	0.267	0.253	0.167	0.167	0.000	0.00
30	0.228	0.218	0.166	0.167	−0.001	− 0.59
35	0.196	0.181	0.165	0.168	−0.003	− 1.78
40	0.166	0.155	0.163	0.165	−0.002	− 1.21
45	0.133	0.127	0.176	0.160	0.016	10.00

TABLE III
Results of Dynamic Mechanical Test for the Nylon 6/CXA 3095 System

Temp (°C)	Measured $E' \times 10^{-9}$ (N/m^2)	Calculated $E' \times 10^{-9}$ (N/m^2)	tan δ_{exp}	tan δ_s	tan δ_{adh}	tan δ_{adh}/tan δ_s (%)
−20	4.037	4.116	0.041	0.035	0.006	17.14
−15	3.538	3.774	0.039	0.037	0.002	5.40
−10	3.218	3.093	0.037	0.040	−0.003	− 7.50
− 5	2.838	3.185	0.036	0.034	0.002	5.88
0	2.533	3.086	0.032	0.033	−0.001	− 3.03
5	2.366	2.781	0.029	0.037	−0.008	−21.62
10	2.153	2.547	0.028	0.039	−0.011	−28.20
15	2.003	2.424	0.027	0.036	−0.009	−25.00
20	1.872	2.118	0.027	0.036	−0.009	−25.00
25	1.779	1.877	0.029	0.035	−0.006	−17.14
30	1.637	1.685	0.033	0.043	−0.010	−23.25
35	1.438	1.493	0.041	0.046	−0.005	−10.86
40	1.320	1.281	0.054	0.056	−0.002	− 3.57
45	1.088	1.017	0.076	0.080	−0.004	− 5.00

TABLE IV
Results of Dynamic Mechanical Test for the Nylon 6/Plexar 3 System

Temp (°C)	Measured $E' \times 10^{-9}$ (N/m²)	Calculated $E' \times 10^{-9}$ (N/m²)	tan δ_{exp}	tan δ_s	tan δ_{adh}	tan δ_{adh}/tan δ_s (%)
−20	5.296	4.430	0.038	0.041	−0.003	− 7.31
−15	4.859	3.962	0.037	0.040	−0.003	− 7.50
−10	3.893	3.237	0.036	0.041	−0.005	−12.19
− 5	3.437	3.275	0.035	0.034	0.001	2.94
0	2.854	3.142	0.033	0.033	0.000	0.00
5	2.662	2.839	0.033	0.036	−0.003	− 8.33
10	2.255	2.596	0.033	0.038	−0.005	−12.16
15	2.023	2.479	0.036	0.036	0.000	0.00
20	1.752	2.167	0.045	0.036	0.009	25.00
25	1.486	1.918	0.061	0.040	0.021	52.50
30	1.197	1.722	0.082	0.043	0.039	90.69
35	0.994	1.526	0.102	0.047	0.055	117.02
40	0.770	1.309	0.127	0.058	0.069	118.96
45	0.596	1.039	0.148	0.081	0.067	82.71

TABLE V
Results of Peeling Test of Coextruded Film[a]

Coextrusion system	Peel strength test (N/cm)
LDPE/EMA	Could not separate
LDPE/Plexar 3	Could not separate
LDPE/CXA 3095	Could not separate
Nylon 6/EMA	1.60
Nylon 6/LDPE	0.18
Nylon 6/Plexar 3	Could not separate
Nylon 6/CXA 3095	Could not separate

[a] The test temperature employed is 25°C.

Figures 20–23 describe the permeability of coextruded composite films, with varying layer thickness ratio. The solid curves in the figures are obtained using the expression (8):

$$\frac{h}{p} = \frac{h_1}{p_1} + \frac{h_2}{p_2} \tag{4}$$

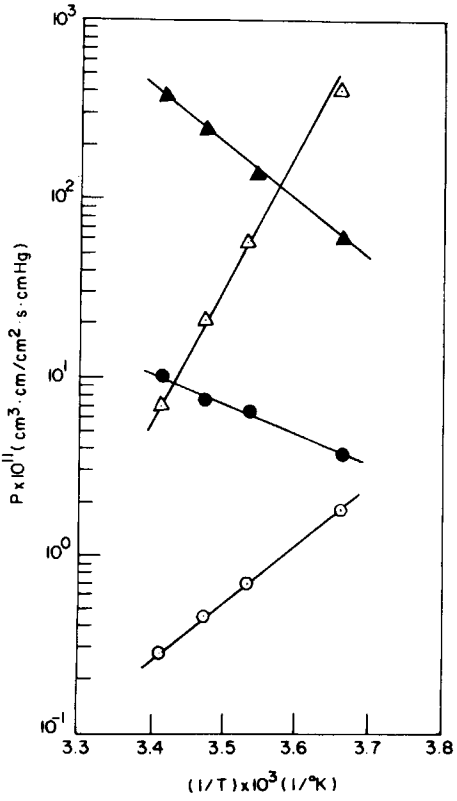

Fig. 18. Temperature dependence of gas permeability: (⊙) N_2 in the nylon 6 film; (△) CO_2 in the nylon 6 film; (●) N_2 in the LDPE film; (▲) CO_2 in the LDPE film.

TABLE VI
Summary of Gas Permeability Test[a]

Polymer system	Permeability × 10^{11} (cm^3 · cm/cm^2 · s · cm Hg)		
	N_2	O_2	CO_2
Nylon 6	0.28	1.11	6.36
Plexar 3	21.40	49.20	680.00
CXA 3095	25.80	61.80	860.00
LDPE	10.40	24.00	355.00
Nylon/Plexar 3[b]	0.35	1.54	12.60
Nylon/CXA 3095[b]	0.53	1.06	6.02
Nylon/LDPE[b]	0.64	2.12	13.26

[a] The test temperature employed is 20°C.
[b] The thickness ratio of the composite film is 1:1.

where h_1 and h_2 are the layer thicknesses of components 1 and 2, respectively, p_1 and p_2 are the permeabilities of components 1 and 2, respectively, h is the total layer thickness ($h_1 + h_2$), and p is the overall permeability of a two-layer composite film. It appears that eq. (4) predicts the permeability of the nylon 6/Plexar 3 composite film (see Figs. 22 and 23) better than it

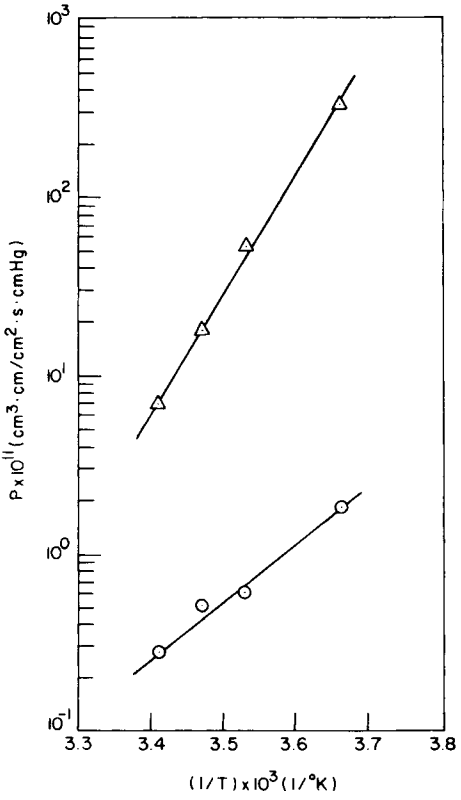

Fig. 19. Temperature dependence of gas permeability in composite films: (⊙) N_2 in the nylon 6/LDPE composite film; (△) CO_2 in the nylon 6/LDPE composite film.

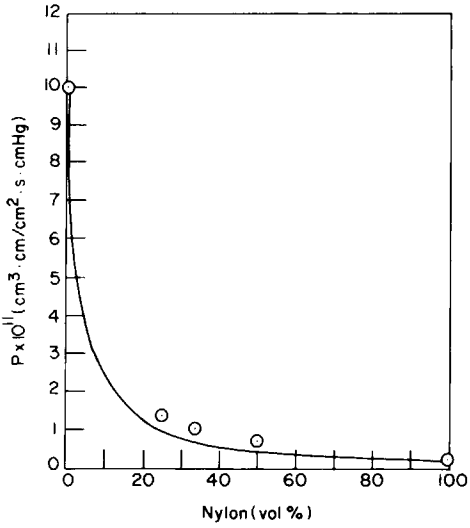

Fig. 20. Composition dependence of the permeability of N_2 in the nylon 6/LDPE composite film at 20°C: (⊙) experimental data; (——) theoretical prediction by eq. (4).

does that of the nylon 6/LDPE composite film (see Figs. 20 and 21). Note that the nylon 6/LDPE composite film has poor adhesion (see Table V).

This study was supported in part by the National Science Foundation under Grant No. ENG-7908513, for which the authors are very grateful. We wish to acknowledge with gratitude that Allied Corp., Chemplex Co., Dow Chemical Co., DuPont Co., and Gulf Oil Chemicals Co. have supplied us with the large quantities of resins used in this investigation.

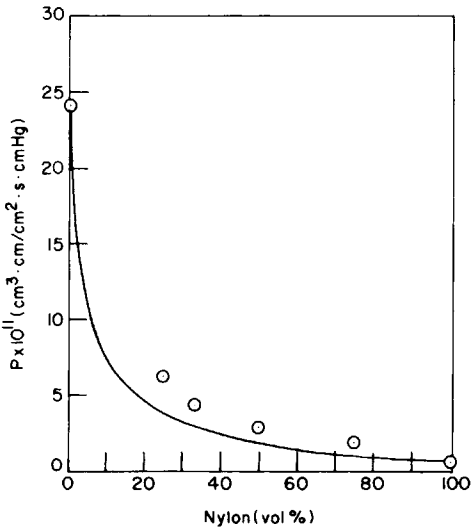

Fig. 21. Composition dependence of the permeability of O_2 in the nylon 6/LDPE composite film at 20°C: (⊙) experimental data; (——) theoretical prediction by eq. (4).

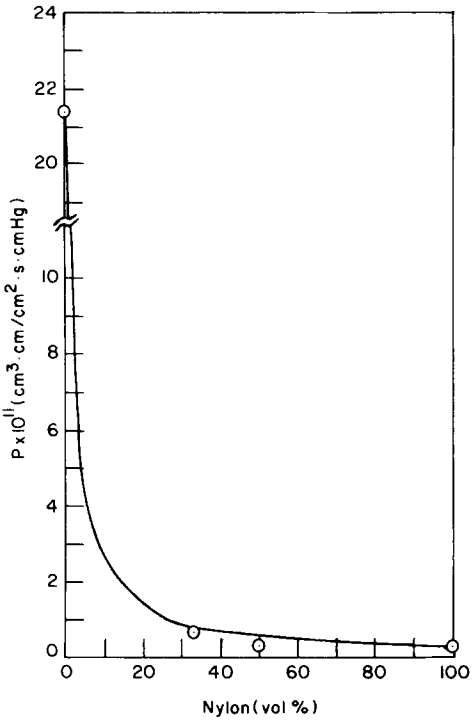

Fig. 22. Composition dependence of the permeability of N_2 in the nylon 6/Plexar 3 composite film at 20°C: (⊙) experimental data; (——) theoretical prediction by eq. (4).

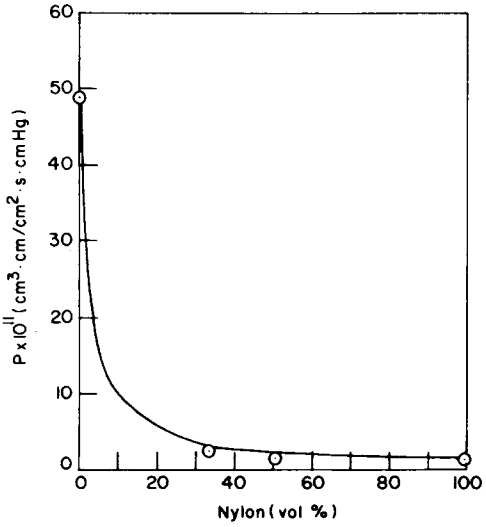

Fig. 23. Composition dependence of the permeability of O_2 in the Nylon 6/Plexar 3 composite film at 20°C: (⊙) experimental data; (——) theoretical prediction by eq. (4).

References

1. Technical brochures, Chemplex Co.
2. Technical brochures, E. I. duPont de Nemours and Co.
3. M. Shida, J. Machonis, S. Schmukler, and R. Zeitlin, 36th ANTEC Prepr. *Soc. Plast. Eng.,* 700 (1978).
4. C. D. Han, *Multiphase Flow in Polymer Processing,* Academic, New York, 1981.
5. C. D. Han, Y. J. Kim, and H. B. Chin, *Polym. Eng. Rev.,* to appear.
6. Y. J. Kim and C. D. Han, *Polym. Eng. Rev.,* **2**, 339 (1983).
7. H. B. Chin, Y. J. Kim, and C. D. Han, *Polym. Eng. Rev.,* to appear.
8. W. J. Schrenk and T. Alfrey, *Polym. Eng. Sci.,* **9**, 393 (1969).
9. N. K. Kalfoglou, *J. Appl. Polym. Sci.,* **22**, 989 (1978).
10. R. A. Dickie and M.-F. Cheung, *J. Appl. Polym. Sci.,* **17**, 79 (1973).
11. K. D. Ziegel and A. Romanov, *J. Appl. Polym. Sci.,* **17**, 1133 (1973).
12. T. B. Lewis and L. E. Nielsen, *J. Appl. Polym. Sci.,* **17**, 1449 (1970).
13. T. Murayama and E. L. Lawton, *J. Appl. Polym. Sci.,* **17**, 669 (1973).
14. C. F. Zorowski and T. Murayama, *Proceedings of the International Conference on Mechanical Behavior of Materials,* Society of Materials Science, Kyoto, 1972, Vol. 5, p. 28.
15. R. Zeitlin, personal communications (1982).

Received February 25, 1983
Accepted December 23, 1983